Applied Physics Letters

Type-II quantum wells with tensile-strained GaAsSb layers for interband cascade lasers with tailored valence band mixing

Cite as: Appl. Phys. Lett. **108**, 101905 (2016); https://doi.org/10.1063/1.4943193
Submitted: 24 January 2016 . Accepted: 22 February 2016 . Published Online: 07 March 2016

M. Motyka, M. Dyksik, K. Ryczko, R. Weih, M. Dallner, S. Höfling, M. Kamp, G. Sęk, and J. Misiewicz

Type-II quantum wells with tensile-strained GaAsSb layers for interband cascade lasers with tailored valence band mixing

M. Motyka,[1] M. Dyksik,[1] K. Ryczko,[1] R. Weih,[2] M. Dallner,[2] S. Höfling,[2,3] M. Kamp,[2] G. Sęk,[1] and J. Misiewicz[1]

[1]*Laboratory for Optical Spectroscopy of Nanostructures, Department of Experimental Physics, Faculty of Fundamental Problems of Technology, Wrocław University of Technology, Wybrzeże Wyspiańskiego 27, Wrocław 50-370, Poland*

[2]*Technische Physik, University of Würzburg, Wilhelm-Conrad-Röntgen-Research Center for Complex Material Systems, Am Hubland, Würzburg D-97074, Germany*

[3]*SUPA, School of Physics and Astronomy, University of St. Andrews, North Haugh, St. Andrews KY16 9SS, United Kingdom*

(Received 24 January 2016; accepted 22 February 2016; published online 7 March 2016)

Optical properties of modified type II W-shaped quantum wells have been investigated with the aim to be utilized in interband cascade lasers. The results show that introducing a tensely strained GaAsSb layer, instead of a commonly used compressively strained GaInSb, allows employing the active transition involving valence band states with a significant admixture of the light holes. Theoretical predictions of multiband k·p theory have been experimentally verified by using photoluminescence and polarization dependent photoreflectance measurements. These results open a pathway for practical realization of mid-infrared lasing devices with uncommon polarization properties including, for instance, polarization-independent midinfrared light emitters.
[http://dx.doi.org/10.1063/1.4943193]

Nowadays, there has been a significant demand for cheap, compact, and easily tunable lasers operating in the midinfrared spectral range. In this respect, semiconductor devices deserve special attention.[1] In particular, lasers emitting at room temperature in the continuous-wave operation mode are of interest for gas sensors in relevant applications such as human breath analysis[2] or detection of harmful or toxic gases, e.g., formaldehyde[3] or nitric oxide.[4] The interband cascade lasers (ICLs)[5,6] have been shown as efficient laser sources for such applications. This was enabled due to their single mode, continuous wave and high power operation at room or even elevated temperatures,[7,8] broad spectral tunability,[9] and low threshold currents resulting in low power consumption.[10]

On the other hand, however, there are still some unresolved issues and space for improvement, where apparently new designs and new material solutions are demanded. One of the fundamental difficulties regarding all the currently considered and utilized type II structures in the ICLs is the wide spectral tuning, which has to be realized with special care for the magnitude of the oscillator strength (OS) of the active optical transition. The wavelength tailoring involves thicker layers used in the active region, which in fact strongly deteriorates the OS due to the influence on electron and heavy hole wave functions separation. In this respect, we would like to explore an additional degree of freedom in designing the laser's active part, involving the light hole states to participate in the fundamental optical transition. This can be realized by using a concept suggested originally by Yang,[11] i.e., employing tensile strained layers of GaAsSb despite commonly used ones of GaInSb. Such an idea based on strain engineering and tuning between the heavy or light hole character of the fundamental transition has recently been elaborated theoretically for type II quantum wells (QWs).[12] In this paper, we focus on its experimental verification and first practical realizations, including the transitions' polarization properties.

We have studied type-II W-design AlSb/InAs/GaAsSb/InAs/AlSb QWs grown on GaSb and InAs substrates, considering the changes in the layers' thickness, the GaAsSb composition, and hence the related strain (differing also depending on the substrate). The electronic and optical properties of the type II QWs with the tensile-strained GaAsSb layer for the confinement of holes appear to be unusual due to the possibility of involving the light hole states, the valence band states mixing, and the following TE/TM (transverse electric/transverse magnetic) polarization control of the fundamental optical transition, leading, for instance, to polarization insensitive emitters. It is worth noticing that some preliminary suggestions on polarization independent emission from interband cascade lasers was reported more than 15 years ago,[13] but never followed by any further developments.

The investigated structures were grown on (100)-oriented GaSb (samples A–C) or InAs (sample D) substrates, in a solid source molecular beam epitaxy system equipped with the valved cracker cells for both antimony and arsenic. The investigated samples were designed as the "W-like" shape quantum wells (see Fig. 1(c)), consisting of two InAs layers and one GaAsSb layer (samples B–D), whereas sample A, as a reference, consisted of two InAs layers and one typically used GaInSb layer. All the QWs' details are listed in Table I, summarizing the structural data based on the high-resolution X-ray diffraction (HR XRD) analysis and the growth calibration procedures.

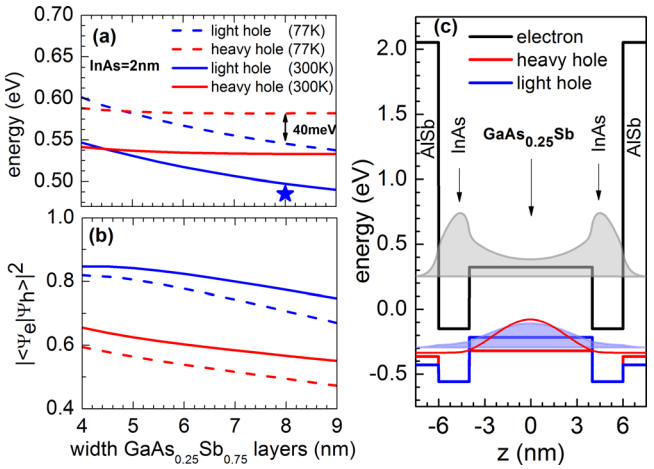

FIG. 1. The calculated energy (panel a) and squared wave function overlap (panel b) for fundamental transition involving heavy (red curves) and light holes (blue curves) in the investigated quantum wells with $GaAs_{0.25}Sb_{0.75}$ layer as a function of layer thickness. Blue star denotes fundamental transition energy measured (by PL) for sample D. Panel c shows band structure together with confining levels and density probabilities of electrons (grey line), light holes (blue line), and heavy holes (red line) for one of the investigated QW (sample D).

The core part of all the samples, i.e., the W-like QW, is surrounded by 2.5 nm thick AlSb barriers. In order to enhance the overall optical response, the wells have been repeated five times and separated from each other by 20 nm of GaSb (samples A–C), or separated by 25 nm thick $GaAs_{0.08}Sb_{0.92}$ layers lattice-matched to InAs (sample D). The entire structure is terminated by the same GaSb or $GaAs_{0.08}Sb_{0.92}$ layer, respectively.

In order to measure photoluminescence (PL) and photoreflectance (PR) in a wide spectral range, we used a setup based on an evacuated Fourier transform (FT) spectrometer Bruker Vertex 80v, operated in a step-scan mode.[14–16] Similar FT-based approaches have been demonstrated as very efficient for optical characterization in the mid-infrared range by several groups.[17–19] In our case, a liquid-nitrogen cooled InSb photodiode was used as a detector. In this measurement configuration, the pump beam was provided by the 660 nm line of a semiconductor laser diode, which was mechanically chopped at a frequency of 275 Hz. Phase sensitive detection of the optical response was performed using a lock-in amplifier.

To calculate the electronic structure of the type-II W-design QWs, we use 8×8 **k·p** Hamiltonian defined for the [001] growth direction.[20,21] The model includes the strain effects after Ref. 22. The carrier wave functions and the subband energies were determined by numerically solving the Schrödinger equation and employing the finite difference method.[23] All material parameters were taken from Ref. 24.

TABLE I. The layer structure of the investigated QWs.

Samples name	Layers confining electrons	Layers confining holes
Sample A	InAs (2 nm)	$Ga_{0.70}In_{0.30}Sb$ (3 nm)
Sample B	InAs (2 nm)	$GaAs_{0.08}Sb_{0.92}$ (8 nm)
Sample C	InAs (4 nm)	$GaAs_{0.08}Sb_{0.92}$ (8 nm)
Sample D	InAs (2 nm)	$GaAs_{0.25}Sb_{0.75}$ (8 nm)

More details on the calculations can be found in our recent theoretical work on that materials' combination in a type II system.[12]

In Figure 1, shown are the calculated fundamental transition energy (panel a) and the squared wave function overlap (panel b) for the type-II AlSb/InAs/GaAsSb/InAs/AlSb QW as a function of GaAsSb layer thickness for a value of As content of 25%. The calculations were performed for 77 K (dashed lines) and 300 K (solid lines). One can see in Fig. 1(a) that when the well width is less than ~5 nm, the fundamental optical transition is of a heavy hole character, whereas for the well width greater than 6 nm, the fundamental transition becomes a light hole transition, when only transitions for $k_{II} = 0$ are considered. It is worth noting that such a situation is a result of the tensile strain in GaAsSb material affecting (via the shear component) the separation of heavy and light hole valence band edges. Such strain shifts the heavy and light hole states in the opposite directions on the energy scale, causing their crossing and final position exchange as a function of the GaAsSb well thickness. In Figure 1, shown are the calculated squared overlaps of the electron and heavy or light hole wave functions for particular transitions showing that the latter is larger for the entire range of the considered GaAsSb layer thicknesses and for the two temperatures considered. To better understand the reasons, exemplary probability densities (calculated for 77 K) are shown in Fig. 1(c) for the case of As content of 25% (i.e., the band diagram corresponding to sample D investigated later experimentally). It is clearly visible that the light hole wave function tunnels much deeper into the InAs layers (when compared to heavy holes), which results in a higher overlap with the electron wave function confined mostly in the InAs layers, however, penetrating significantly into the separating GaAsSb layer.

In Figure 2, the normalized photoluminescence spectra are shown for all the investigated samples. In all cases, the emission from the type II quantum wells could be detected at room temperature, which indicates a good optical quality. The spectral position of the PL peaks shifts depending on the

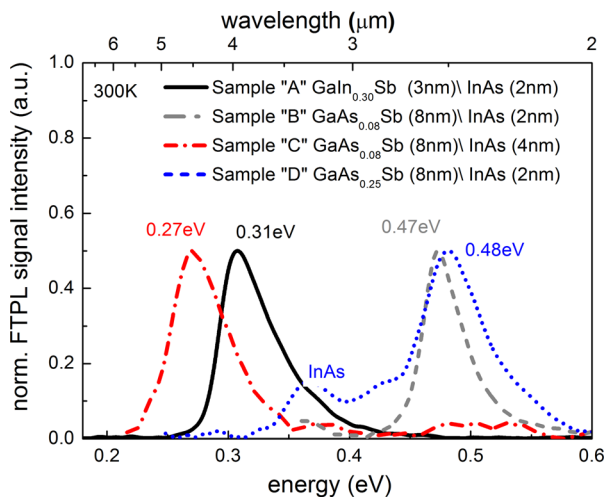

FIG. 2. Room temperature Fourier transformed photoluminescence of the type-II W-design AlSb/InAs/$GaAs_xSb_{1-x}$/InAs/AlSb QWs with different As content and layers thickness. Black solid line corresponds to the reference QW with GaInSb layer.

layer structure details. In addition, for sample D, the signal from InAs substrate was detected around 0.36 eV.

Figure 3 shows a comparison between the calculated transition energies (plotted in function of the InAs layer thickness) and the experimental values from the PL spectra. As it can be seen, a very good agreement has been obtained. Starting from the reference sample with the fundamental transition at around 0.3 eV, we have modified the active region with the involvement of different GaAsSb layers to get various transition energies (from around 0.5 to below 0.3 eV). The contents of 8% of arsenic in GaAsSb QW do not change the character of the fundamental transition, which still remains of heavy hole type, as in the reference structure.[11] For such a content (according to our calculations—not shown here), the light hole states are becoming unconfined, making it difficult to detect them in optical spectra. For this reason, further investigations were focused only on sample D, for which the As content in the GaAsSb layer was determined to be 23%–26% taken from XRD profile analysis (well agreed with the nominal value of 25%). In such a case, the energy difference between the light and heavy holes levels is about 40 meV (see Fig. 1(a)—indicated by an arrow), and both are well confined, which allows for further possibility to measure transitions involving these states in, for instance, the modulation spectroscopy. Note that for sample D and when regarding room temperature PL, good agreement between calculations and experiment was also obtained (see the blue star in Fig. 1(a)). Additionally, the measured PL peak energy compared to the calculated values suggests the light hole character of the fundamental transition, as expected. For experimental verification of the character of the transitions, the linear-polarization-resolved photoreflectance measurement was used.

Figure 4(a) shows the Fourier-transformed photoreflectance spectra for the type-II AlSb/InAs/$GaAs_{0.25}Sb_{0.75}$/InAs/AlSb QW (sample D) obtained for different probing light polarization in the range from 0° (TE-polarization) to 90° (TM-polarization), respectively, and measured at 77 K. In these experiments, the incidence angle for the probe beam

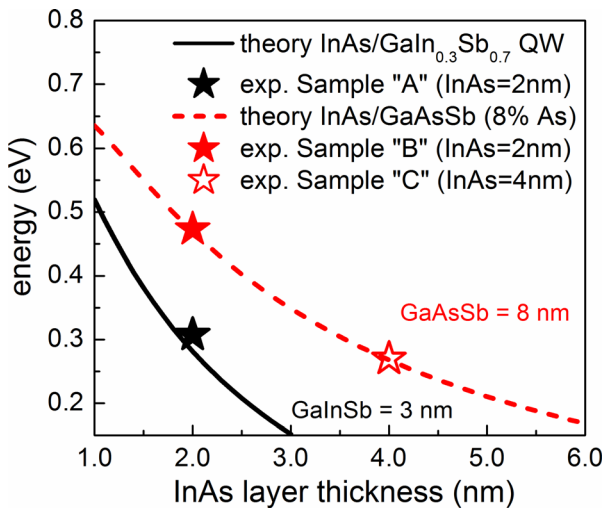

FIG. 3. The calculated energies (curves) of the fundamental transition in investigated QWs as a function of InAs thickness together with experimental values (stars) taken from PL measurement.

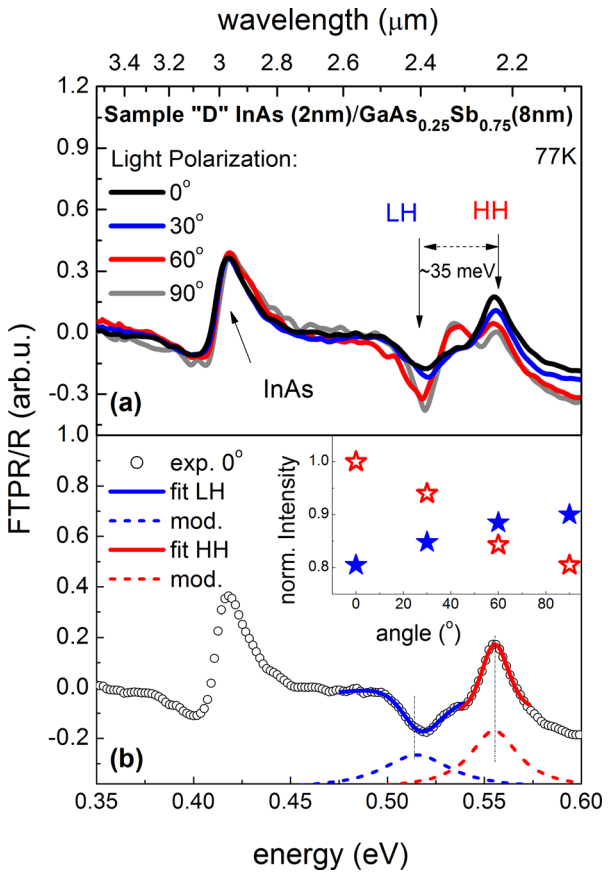

FIG. 4. Polarization dependence of the photoreflectance spectra measured for sample D (panel a). An example of the performed analysis for spectra obtained for TE-light polarization. The inset shows signals intensity in function of the light polarization for light (solid symbols) and heavy (open symbols) holes related transitions.

was 45°, for which the selection rules allow detecting the varying ratio of TE and TM components for the particular transitions. For all the measurements, we can distinguish a signal at 0.410 eV, which is connected with the InAs energy gap transition, and two features at ~0.520 eV and ~0.555 eV, which we relate to the type II QW. The determined energy difference between these two spectral lines is around 35 meV, which agrees well with the calculated and abovementioned light hole-heavy hole splitting in the valence band.

Figure 4(b) shows the results of fitting procedure for one of the measured spectra (TE light polarization)—assuming the PR line-shape according to the commonly used formula[25,26]

$$\frac{\Delta R}{R}(E) = \mathrm{Re}\left[\sum_{j=1}^{n} C_j \cdot e^{i\cdot\vartheta_j}(E - E_j + i\cdot\Gamma_j)^{-m_j}\right], \quad (1)$$

where n is the number of optical transitions and independent spectral functions used in the fitting procedure, C_j and ϑ_j are the amplitude and phase parameters, E_j and Γ_j are the energy and the broadening parameter of the transitions, respectively, whereas m is a parameter depending on the type of optical transition. The m parameter has been used equal 3, as such a lineshape imitates well the modulated reflectivity spectra for the confined states transitions.[27] The other fitting parameters

are not discussed because they are not relevant for the main purpose, which is determination of the transition intensities versus polarization. The fitting curves are shown together with the moduli of the individual resonances (dashed lines) obtained according to following equation:

$$\Delta\rho(E) = \frac{|C|}{\left[(E - E_0)^2 + \Gamma^2\right]^{\frac{m}{2}}}. \quad (2)$$

Such an approach allowed obtaining information about the polarization dependence of the intensity for both measured QW transitions. As we can see in the inset of Fig. 4, when the polarization changes from 0° to 90°, the intensity of the lower energy transition increases, whereas the intensity of the higher energy signal decreases. This is a typical behavior for light and heavy hole related transitions in QWs.[28] Due to the opposite dependence of the intensity as a function of light polarization, the signals were ascribed as light and heavy holes related. The calculated energies for the type II AlSb/InAs/$GaAs_{0.25}Sb_{0.75}$/InAs/AlSb QW as a function of GaAsSb thickness were already shown in Figure 1(a). Although the absolute values are slightly shifted with respect to the experimental ones, the heavy hole–light hole energy separation of 40 meV confirms the abovementioned interpretation. The discrepancy of about 30 meV for the absolute values of the transition energies between the calculation and experiment can be related to some uncertainties in the As content, the PR fit procedure, and finite layer thicknesses accuracy.

All these considerations show that a proper As content and layer widths engineering in such structures can switch the character of the valence band states involved in the fundamental optical transition. In a particular case, we can imagine, that the contributions of the heavy and light hole states are so, that the resulting emission intensities in TE and TM polarizations can be equal. In Figure 5, we have shown the calculated energies of the heavy hole and light hole states and their contribution to the topmost valence subband wave function. The calculations were performed as a function of k_{II} in the [10] in-plane direction. The composition of the

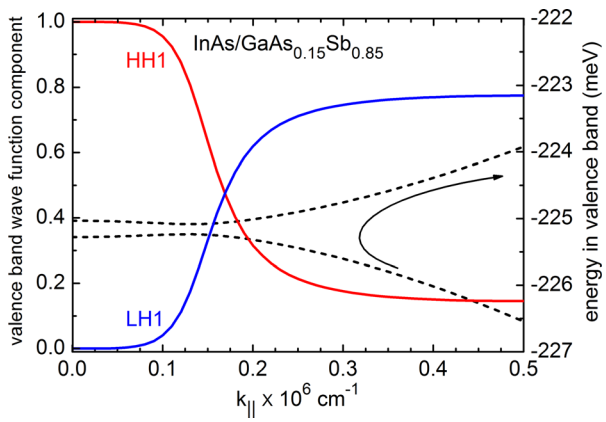

FIG. 5. The calculated energies of the two lowest levels states (dashed lines—right axis) in type II AlSb/InAs/$GaAs_{0.15}Sb_{0.85}$/InAs/AlSb QW as a function of k_{II} wave vector corresponding to the [10] in-plane direction, together with calculated contributions to the valence band wave function for the topmost valence subband (solid lines—left axis).

layer confining holes was chosen around 15% of arsenic to keep the two lowest heavy and light holes levels very close to each other in a broad k_{II}-space range (see the dashed lines in Fig. 5). Analyzing the wave function components, we can see that the light-hole contribution increases for larger k_{II} vectors in our case when the fundamental valence band state has the heavy-hole character at $k_{II} = 0$. Additionally, we can easily see that there is a point in k_{II}-space, where both the wave function contributions might be equal. The analysis out of $k_{II} = 0$ is crucial when such QWs are placed in the active region of the lasing devices, and the high carrier concentrations make necessary the consideration of the filled up subbands. It has to be also mentioned that, in general, for the proper prediction on the polarization-independence, the in-plane anisotropy should be taken into account. However, in the considered case and according to our calculations, it appeared to be insignificant in the given range of the wave numbers where the strong heavy hole–light hole mixing occurred. Independently of that, these results show the possible ways of optimization in such tensile-strained structures, which allows designing the emission polarization properties including, for instance, a fully polarization independent interband cascade laser.

We have performed optical measurements on a set of type II QW samples utilizing a GaAsSb layer instead of commonly used GaInSb. The properly chosen widths of the layers, together with strain engineering provided by changing the arsenic content of the GaAsSb wells, allowed involving the light holes states into the fundamental optical transition. On one hand, this approach provided an additional degree of freedom for the emission wavelength transition oscillator strength tuning. On the other hand, the obtained results show that this type of the active region utilizing light holes related emission might be an interesting approach for the design and fabrication of the polarization-controlled mid-infrared light emitters.

This project has received funding from the European Union's Horizon 2020 research and innovation programme under grant agreement No 636930. We would also like to acknowledge the National Science Centre of Poland for support within Grant No. 2014/15/B/ST7/04663.

[1]A. Bauer, K. Rößner, T. Lehnhardt, M. Kamp, S. Höfling, L. Worschech, and A. Forchel, Semicond. Sci. Technol. **26**, 014032 (2011).
[2]T. H. Risby and F. K. Tittel, Opt. Eng. **49**, 111123 (2010).
[3]S. Lundqvist, P. Kluczynski, R. Weih, M. v. Edlinger, L. Nähle, M. Fischer, A. Bauer, S. Höfling, and J. Koeth, Appl. Opt. **51**, 6009–6013 (2012).
[4]M. von Edlinger, J. Scheuermann, R. Weih, C. Zimmermann, L. Nähle, M. Fischer, J. Koeth, and S. Höfling, IEEE Photonics Technol. Lett. **26**, 480 (2014).
[5]R. Q. Yang, Superlattices Microstruct. **17**, 77 (1995).
[6]I. Vurgaftman, R. Weih, M. Kamp, J. R. Meyer, C. L. Canedy, C. S. Kim, M. Kim, W. W. Bewley, C. D. Merritt, J. Abell, and S. Höfling, J. Phys. D: Appl. Phys. **48**, 123001 (2015).
[7]W. W. Bewley, C. S. Kim, C. L. Canedy, C. D. Merritt, I. Vurgaftman, J. Abell, J. R. Meyer, and M. Kim, Appl. Phys. Lett. **103**, 111111 (2013).
[8]C. S. Kim, M. Kim, J. Abell, W. W. Bewley, C. D. Merritt, C. L. Canedy, I. Vurgaftman, and J. R. Meyer, Appl. Phys. Lett. **101**, 061104 (2012).
[9]Y. Jiang, L. Li, Z. Tian, H. Ye, L. Zhao, R. Q. Yang, T. D. Mishima, M. B. Santos, M. B. Johnson, and K. Mansour, J. Appl. Phys. **115**, 113101 (2014).

[10]I. Vurgaftman, W. W. Bewley, C. L. Canedy, C. S. Kim, M. Kim, C. D. Merritt, J. Abell, J. R. Lindle, and J. R. Meyer, Nat. Commun. **2**, 585 (2011).
[11]R. Q. Yang, in *Long Wavelength Infrared Emitters Based on Quantum Wells and Superlattices*, edited by M. Helm (Gordon and Breach, Singapore, 2000), Chap. 2.
[12]K. Ryczko, G. Sęk, and J. Misiewicz, Appl. Phys. Express **8**, 121201 (2015).
[13]E. Dupont, H. C. Liu, and R. Q. Yang, J. Appl. Phys. **89**, 7195 (1999).
[14]M. Motyka, G. Sęk, J. Misiewicz, A. Bauer, M. Dallner, S. Höfling, and A. Forchel, Appl. Phys. Express **2**, 126505 (2009).
[15]M. Motyka and J. Misiewicz, Appl. Phys. Express **3**, 112401 (2010).
[16]M. Motyka, G. Sęk, F. Janiak, J. Misiewicz, K. Kłos, and J. Piotrowski, Meas. Sci. Technol. **22**, 125601 (2011).
[17]T. J. C. Hosea, M. Merrick, and B. N. Murdin, Phys. Status Solidi A **202**, 1233 (2005).
[18]J. Shao, W. Lu, F. Yue, X. Lu, W. Huang, Z. Li, and S. Guo, Rev. Sci. Instrum. **78**, 013111 (2007).
[19]D. D. Firsov and O. S. Komkov, Tech. Phys. Lett. **39**, 1071–1073 (2013).
[20]K. Ryczko, G. Sęk, and J. Misiewicz, J. Appl. Phys. **114**, 223519 (2013).
[21]H. R. Trebin, U. Rössler, and R. Ranvaud, Phys. Rev. B **20**, 686 (1979).
[22]L. Bir and G. E. Pikus, *Symmetry and Strain-Induced Effects in Semiconductors* (Wiley, New York, 1974).
[23]J. W. Thomas, *Numerical Partial Differential Equations: Finite Difference Methods* (Springer-Verlag, New York, 1995).
[24]I. Vurgaftman, J. R. Meyer, and L. R. Ram-Mohan, J. Appl. Phys. **89**, 5815 (2001).
[25]F. H. Pollak, in *Modulation Spectroscopy of Semiconductors and Semiconductor Microstructures Handbook on Semiconductors*, edited by T. S. Moss (Elsevier Science, Amsterdam, 1994), Vol. 2, pp. 527–635.
[26]D. E. Aspnes, Surf. Sci. **37**, 418 (1973).
[27]B. V. Shanabrook, O. J. Glembocki, and W. T. Beard, Phys. Rev. B **35**, 2540 (1987).
[28]G. Bastard, *Wave Mechanics Applied to Semiconductor Heterostructures* (Les Editions de Physique, 1988).